Geophysical Research Letters

RESEARCH LETTER
10.1029/2018GL079787

Key Points:
- Englacial water storage was observed in damaged solid ice with a phase-sensitive radar in the ablation zone of Store Glacier, West Greenland
- Englacial water storage, intercepting a portion of surface meltwater, may contribute to the observed variability in glacial flow behavior
- Coincident periodic subglacial drainage events indicate an active subglacial drainage network beneath the englacial storage

Supporting Information:
- Supporting Information S1

Correspondence to:
A. K. Kendrick,
alexkend@stanford.edu

Citation:
Kendrick, A. K., Schroeder, D. M., Chu, W., Young, T. J., Christoffersen, P., Todd, J., et al. (2018). Surface meltwater impounded by seasonal englacial storage in West Greenland. *Geophysical Research Letters*, *45*. https://doi.org/10.1029/2018GL079787

Received 30 JUL 2018
Accepted 20 SEP 2018
Accepted article online 24 SEP 2018

Surface Meltwater Impounded by Seasonal Englacial Storage in West Greenland

A. K. Kendrick[1], D. M. Schroeder[1,2], W. Chu[1], T. J. Young[3,4], P. Christoffersen[3], J. Todd[3,5], S. H. Doyle[6], J. E. Box[7], A. Hubbard[6,8], B. Hubbard[6], P. V. Brennan[9], K. W. Nicholls[4], and L. B. Lok[9]

[1]Department of Geophysics, School of Earth, Energy and Environmental Sciences, Stanford University, Stanford, CA, USA, [2]Department of Electrical Engineering, School of Engineering, Stanford University, Stanford, CA, USA, [3]Scott Polar Research Institute, University of Cambridge, Cambridge, UK, [4]British Antarctic Survey, Cambridge, UK, [5]Department of Geography and Sustainable Development, University of St Andrews, St Andrews, UK, [6]Centre for Glaciology, Department of Geography and Earth Sciences, Aberystwyth University, Aberystwyth, Ceredigion, UK, [7]Glaciology and Climate, Geological Survey of Denmark and Greenland, Copenhagen, Denmark, [8]Centre for Arctic Gas Hydrate, Environment and Climate, Department of Geology, University of Tromsø, Tromsø, Norway, [9]Department of Electronic and Electrical Engineering, University College London, London, UK

Abstract The delivery of surface meltwater through englacial drainage systems to the bed of the Greenland Ice Sheet modulates ice flow through basal lubrication. Recent studies in Southeast Greenland have identified a perennial firn aquifer; however, there are few observations quantifying the input or residence time of water within the englacial system and it remains unknown whether water can be stored within solid ice. Using hourly stationary radar measurements, we present observations of englacial and episodic subglacial water in the ablation zone of Store Glacier in West Greenland. We find significant storage of meltwater in solid ice damaged by crevasses extending down to 48 m below the ice surface during the summer, which is released or refrozen during winter. This is a significant hydrological component newly observed in the ablation zone of Greenland that could delay the delivery of meltwater to the bed, changing the ice dynamic response to surface meltwater.

Plain Language Summary Surface meltwater can drastically modify how glaciers flow. Depending on how and when it is delivered, meltwater can cause variable motion by modulating friction at the ice sheet base. Englacial water can control this behavior by either preventing water from reaching the bed or by delaying its release. In this paper, we present detailed observations of water storage within and at the bed of Store Glacier in West Greenland using hourly stationary ice penetrating radar measurements. In contrast to the previously discovered firn aquifer in high-accumulation regions, at Store Glacier englacial water is present within a region of solid, damaged ice and persists until winter. This type of water storage has not been previously observed in solid ice and could explain some of the complex flow behavior of some Greenland glaciers.

1. Introduction

Meltwater drainage from the surface to the bed along the margin of the Greenland Ice Sheet produces transient ice velocity fluctuations by enhancing basal sliding through hydraulic pressurization (Andrews et al., 2014; Bartholomew et al., 2012; Schoof, 2010; Zwally et al., 2002). However, this effect is not fully understood, with surface velocity measurements often displaying a contrasting relationship with meltwater input. For example, comparable surface meltwater production on the same glacier can lead to notable flow acceleration in 1 year and produce a diminished velocity response in another (Fitzpatrick et al., 2013; Joughin et al., 2013; Moon et al., 2014). This variation across Greenland is likely closely linked to the flow, storage, and distribution of water among and within the englacial and subglacial drainage systems (Andrews et al., 2014; Bartholomew et al., 2012; Sole et al., 2011).

To date, most hydrological studies have focused on either supraglacial or subglacial drainage (Andrews et al., 2014; Bartholomew et al., 2012; Smith et al., 2015). These studies demonstrate that switches in the configuration of subglacial drainage between efficient and inefficient systems are partly responsible for the observed complex velocity response (Bartholomew et al., 2012; Chu et al., 2016; Schoof, 2010; Sole

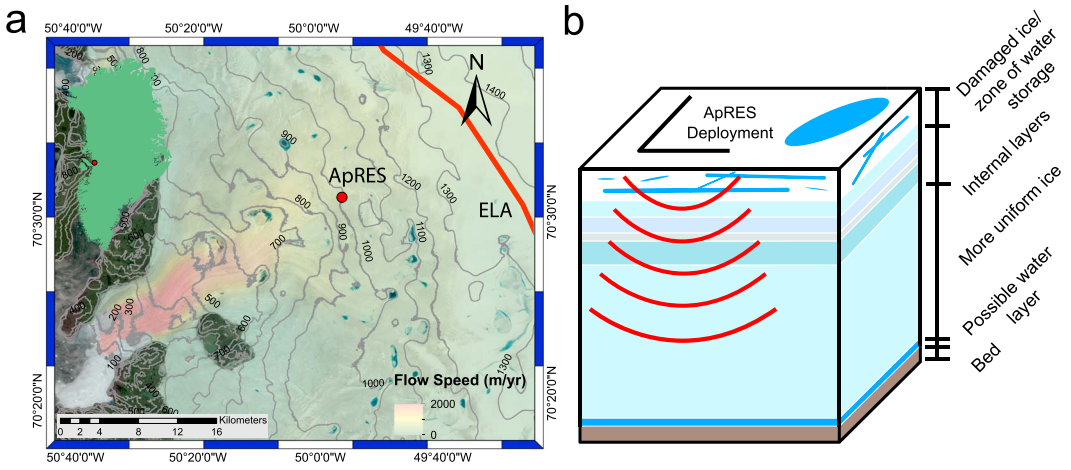

Figure 1. (a) Landsat-8 image of Store Glacier from 1 July 2014 showing the location of the ApRES deployment and the position of the deployment relative to Greenland, overlain by winter MEaSUREs ice flow velocity for 2014–2015 derived from InSAR data (Joughin et al., 2015). The red line indicates the equilibrium line altitude (ELA). Elevation contours were generated using ArcticDEM release 6. DEM created by the Polar Geospatial Center from DigitalGlobe, Inc., imagery. (b) Schematic of ApRES deployment on Store Glacier. The presence of water within the ice column imaged by ApRES will attenuate the measured echoes from both the internal layers and the bed. Water at the basal interface will modify the basal reflectivity, further modifying the bed echo.

et al., 2011). Recent studies in Southeast Greenland have also highlighted the importance of a perennial englacial firn aquifer and its unknown role in modulating ice dynamics (Forster et al., 2013; Koenig et al., 2014; Miège et al., 2016; Miller et al., 2017; Montgomery et al., 2017). Englacial aquifers provide long-term storage of meltwater, potentially reducing the proportion of surface water reaching the bed. Thermal observations have also identified similar meltwater retention in the accumulation area in West Greenland (Humphrey et al., 2012). Despite its importance, observations of englacial storage are mostly limited to firn in high accumulation regions, with only a few observations of storage within the bare ice zones (Cooper et al., 2018). The prevalence of water storage outside the permeable firn regions and the fraction of annual meltwater stored in bare ice remains unknown.

We present simultaneous observations of the englacial and subglacial water systems of Store Glacier, Greenland using a high-resolution, low-power, autonomous phase-sensitive radio-echo sounder (ApRES). The ApRES system is a ground-based frequency-modulated continuous wave radar that operates across the 200–400 MHz frequency range (Brennan et al., 2014). While similar systems have been previously deployed in Antarctica to quantify rapid variations in vertical strain (Kingslake et al., 2014) and basal melt rates (Nicholls et al., 2015), we present the first study that utilizes the full temporal resolution of ApRES measurements to characterize and quantify englacial water storage.

2. Materials and Methods

2.1. ApRES Deployment and Data Processing

An ApRES system was deployed at Store Glacier in Western Greenland ~15 km downstream of the equilibrium line altitude during two periods from 9 May 2014 to 16 July 2014 and 4 August 2014 to 30 November 2014 and measured simultaneous changes in meltwater storage for both englacial and subglacial drainage systems (Figure 1; Young et al., 2018). At this location, the ice is between 600–650 m thick and the glacier experiences seasonal changes in ice flow velocities ranging from ~600 m/a in the winter to ~700 m/a during the melt season. We process the ApRES data and generate a set of 2-D cross sections of radar echo power from the top to bottom of the ice sheet every 1 hr (May–July) and 4 hr (August-November; Figure 2). Variation in echo power from identified internal ice layers and the bed provides observational constraints on changes in englacial and subglacial water storage with subdaily temporal resolution. The presence of englacial water within the ice can dramatically increase volumetric scattering and attenuates received

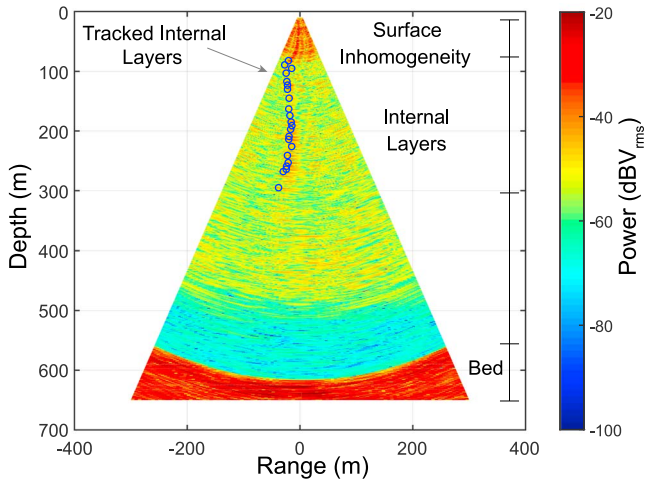

Figure 2. Example 2-D ApRES cross section from 9 May 2014 showing the location of the identified internal layers (blue circles) tracked from May to July 2014. The internal layers were identified as the strong reflectors present in the upper 300 m of ice (Young et al., 2018). Below 300 m, little internal structure is visible before the strong bed echo at about 617 m. Similar features were identified as internal layers and tracked during deployment 2 from August to November 2014.

radar signals, decreasing the return power of internal layers and bed echoes. We utilize the attenuating properties of englacial water to constrain how englacial water storage changes throughout our study period on Store Glacier.

In order to identify temporal changes in radar attenuation, we track the power of strong reflectors identified in the 2-D ApRES cross sections. These features likely correspond to internal layers beneath the region of both ApRES deployments (Young et al., 2018). We track 22 features as internal layers every hour throughout deployment 1 of the ApRES array from 9 May 2014 to 16 July 2014 and of 21 features every 4 hrs during deployment 2, from 4 August 2014 to 30 November 2014. The ApRES array was relocated approximately 400 m upglacier and rotated by 12° relative to the principal flow direction between deployments 1 and 2 (supporting information Figure S1). We apply a constant correction to calibrate the systematic offsets in radar echo power between the two deployments by performing a linear fit to the average power of the internal layers at the end of deployment 1 and the start of deployment 2. By taking the slope of the mean internal layer power (−0.88 dB/day during deployment 1 and −0.84 dB/day in deployment 2) a constant offset of −38.49 dB was needed to calibrate the echo power values for deployment 2 that began 19 days later.

2.2. Modeling Radar Attenuation From Englacial Water Storage

Englacial water storage will increase the observed radar attenuation depending on the amount and electrical conductivity of the water (Schroeder et al., 2015). For centimeter-scale pores, volumetric scattering will also increase radar attenuation by an amount depending on the porosity of the englacial storage and average pore size (Aglyamov et al., 2017; Bohren & Huffman, 1983; Ulaby et al., 2014). To forward model the expected radar attenuation we estimate the two-way attenuation through the region of water storage according to its skin depth,

$$A = e^{-\frac{2T}{\delta}} \tag{1}$$

where A is attenuation, T is the thickness of the region of water storage, and δ is the skin depth. The skin depth is given by

$$\delta = \sqrt{\frac{1}{\pi f_c \sigma_{ws} \mu_0}} \tag{2}$$

where f_c is the center frequency of the radar, σ_{ws} is the conductivity of the region of water storage, and μ_0 is the permeability of free space (Schroeder et al., 2015). Estimates of cumulative mass loss estimated by the RACMO2.3p2 1-km surface mass balance (SMB) model (Noël et al., 2018) are used to approximate the amount of accumulated liquid water for the ApRES deployment period. We calculate the thickness of the region required to store the estimated accumulated water, T, for a given porosity, φ. Using a mixing model previously designed and applied to estimate the electrical conductivity of sea ice (Geldsetzer et al., 2009), we calculate the conductivity of englacial water storage given by

$$\sigma_{ws} = \sigma_w(\varphi - \varphi_c)^y \tag{3}$$

where σ_w is the surface water conductivity, φ is the water volume fraction (porosity), φ_c is the volume fraction limit below which the connectivity of conductive pores can be ignored, and y is an empirical parameter that controls the increase in conductivity for volume fractions above φ_c. Following previous work, we set $\varphi_c = 0$ and $y = 1.67$ (Clarke et al., 1978; Geldsetzer et al., 2009).

We use an open source MATLAB Mie scattering solver (Bohren & Huffman, 1983; Mätzler, 2002) for homogeneous spheres to model volume scattering. The calculated scattering efficiency of water-filled pores of a given radius, r, within an ice column is used to estimate the two-way scattering losses (Aglyamov et al., 2017). The index of refraction of ice (Warren & Brandt, 2008) and water (Segelstein, 1981) at a wavelength

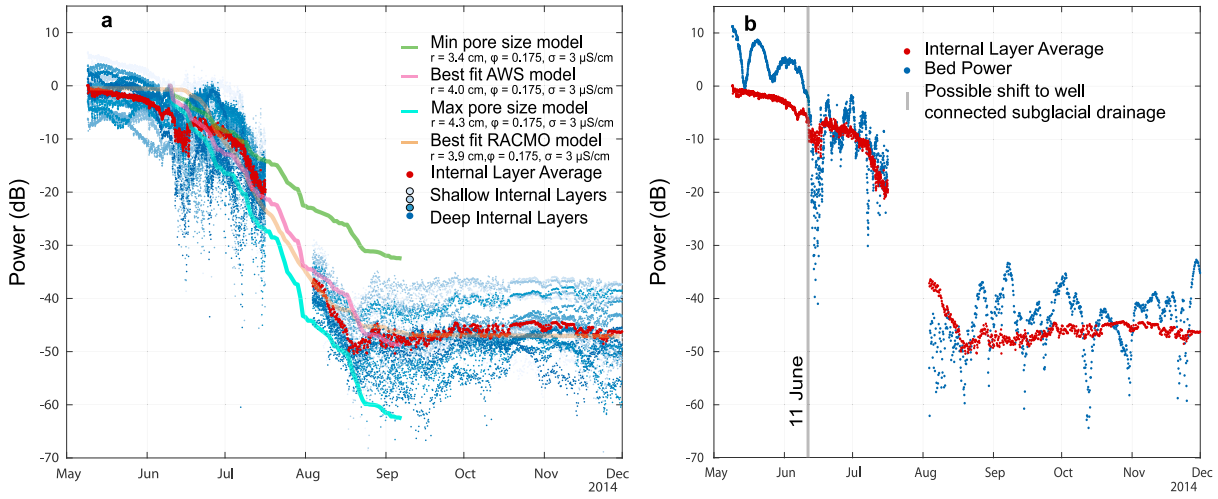

Figure 3. (a) Observed ~45-dB reduction in returned power from identified internal layers from 9 May to 7 September overlain with predicted attenuation curves using the observed AWS surface melt record near the ApRES deployment and cumulative mass loss as predicted by RACMO2.3p2 1-km SMB as an estimate of surface melt. Power returned by internal layers are colored according to depth. As the most sensitive parameter, attenuation models are shown for a range of r = 3.4–4.3 cm using a mean, $\varphi = 0.175$, and $\sigma = 3$ μS/cm. (b) Observed bed power superimposed on the internal layer average. Periodic variations in bed power are observed between May and early June providing evidence of subglacial water. These periodic variations become more sporadic after 11 June possibly indicating a transition from a poorly to well-connected subglacial system.

of 100 cm were used to estimate the scattering efficiency. The minimum (3.4 cm) and maximum (4.3 cm) pore radius were estimated by forward modeling attenuation using mean estimates of conductivity and porosity, 0.175 and 3 μS/cm.

To estimate the thickness of the englacial storage region from the data, we reverse the above equations to forward model radar attenuation and estimate T for a given φ, σ_w, and r based on the observed ApRES attenuation (Figure S2). Since the fraction of attenuation resulting from volume scattering is independent of T, we can quantify the attenuation resulting from water storage. The estimates of water storage required to produce the observed attenuation are then compared with surface melt measured by an automatic weather station (AWS) installed within 1 km of the ApRES deployment and estimates of cumulative mass loss from the RACMO2.3p2 1-km SMB.

3. ApRES Observations

The observed time series of radar profiles reveals substantial seasonal changes in both the internal layer and bed echo power (Figure 3). Within the ice, the internal layer echo strength decreases by 45 dB from May to December (Figure 3a). This decrease is gradual in the early season with ~8 dB of change between May and the end of June. Before significant surface melting occurs, we observe ~1 dB diurnal variations in internal layer power likely due to surface temperature variations. Later in the season, the internal layer power reduces by ~35 dB between July and September. Notably, the internal layer power remains low until the end of our observational record in December. Across both deployments, the observed layer attenuation signal has no depth dependence (Figure 3a), suggesting the source of the power variation impacts all internal layers equally. This indicates that any possible feature responsible for the decrease in power is located above the identified internal layers in the region of surface inhomogeneity as shown in Figure 2 such that the returned signal from all of the strong reflectors passes through this feature. Over the same period, we also observe periodic fluctuations at 10–15 dB in bed echo power superimposed on the same background attenuation signal as the layers (Figure 3b). These oscillations are well defined before 11 June before becoming more sporadic later in the season.

4. Discussion

4.1. Evidence of Englacial Water Storage

We interpret the 45 dB decrease in both the internal layers and bed echo power to be a result of the formation of near-surface englacial water storage. Neither instrumental power nor seasonal temperature variations

could produce a large enough attenuation signal to explain our observed radar power loss in the internal layers.

Penetration of warm summer air temperatures through the ice sheet could affect the upper ice column temperatures through heat conduction (Cuffey & Paterson, 2010). A warming of 1 °C in the ice column would increase the englacial attenuation by ~ 1–5 dB km^{-1} and would reduce the internal layer power (MacGregor et al., 2015). To estimate a worst-case scenario, we consider a theoretical temperature swing of 40 °C between the end of March and mid-July. By applying this value in an energy balance model (Hooke, 2005), we estimate an average ice temperature increase of 2.4 °C localized in the top 15 m of an ice column at the ApRES site. We propagate this temperature change through a radar attenuation model (MacGregor et al., 2007, 2015, Matsuoka et al., 2010, 2012) and calculate an upper-bound estimate of the cumulative change in englacial attenuation of less than 1 dB between May and December through the top 50 m of ice. Variations in the ice column temperature alone cannot explain the substantial 10- to 45-dB reduction in internal layer power. Similarly, a systematic decrease in transmit power is also unlikely to be responsible for the observed reduction in internal layer power. The battery voltage of the ApRES array is stable for both deployments, gradually decreasing by ~0.2 V over 3–4 months.

Stored englacial water increases scattering losses and englacial attenuation as a function of pore radius, volume, and electrical conductivity. Therefore, we can use the observed attenuation to further constrain the properties and configuration of the englacial storage. For our initial assessment of englacial storage, we use a range of porosities from 0.05 to 0.3 based on previous observations (Cooper et al., 2018; Koenig et al., 2014) and a range of meltwater conductivities of 1.6–4.4 μS/cm from an englacial profile through a borehole adjacent to the ApRES deployment (Doyle et al., 2018). For this range of conductivity and porosity, we estimate water storage in macroporous ice between 3.4 and 4.3 cm in radius is responsible for the observed attenuation in Figure 3a. To place conservative bounds on the minimum and maximum englacial storage fraction and to capture the uncertainty inherent in our model parameters, we estimate water storage for each combination of these parameters (Table S1). Although the specific combination of conductivity, porosity, and water volume that predicts the observed attenuation is nonunique, this model demonstrates that the observed attenuation signal is consistent with storing a significant fraction of the observed surface melt.

We estimate that 1.3–2.6 m of surface meltwater is stored in a macroporous ice layer between 4.6 and 45.0 m thick. Our estimates of a 4.6- to 45.0-m-thick porous layer are comparable to the 7.7- to 37.8-m-thick firn aquifer previously identified at Helheim Glacier in Southeast Greenland (Koenig et al., 2014; Miller et al., 2017). However, unlike the firn aquifer, we found no distinctive bright reflector within the ice column or any loss of radar bed echoes directly beneath the englacial storage at our study site (Figure S3; Leuschen, 2014). This indicates that englacial storage in the bare ice region of Store Glacier is distinctly different from the perennial firn aquifer observed on the high accumulation region on Helheim Glacier (Forster et al., 2013). Instead, we associate our observed water storage with a porous layer of damaged solid ice, resulting from fast and extensional glacier flow and surface crevasses extending to an estimated depth between 44 and 48 m at the ApRES deployment (Figure S1; Todd et al., 2018). Our observations suggest more water is stored than is currently plausible in 1–2 m of weathered crust (Cooper et al., 2018), but it could be possible a thick region of weathered ice has accumulated beneath the ApRES deployments. This region of macroporous or damaged ice likely extends laterally over an area of at least 400 m encompassing both deployments 1 and 2 as both locations exhibit the same attenuation signal (Figure S1).

4.2. Comparing Observed Storage to Seasonally Available Local Surface Melt

The englacial storage of 1.3–2.6 m of water between May to December represents a significant portion of the 1.9 m of surface melt production determined from AWS data acquired at the ApRES deployment site and confirmed by ablation stake measurements. These observations are validated by regional climate model (RACMO2.3p2; Noël et al., 2018) estimates of surface water budget that suggests a cumulative SMB loss of 1.9 m, runoff of 2.1 m, and surface melt of 2.4 m. The bulk of mass loss and positive temperature events occur over a 3-month span ranging from 1 June to 9 September (Figure S4). The cumulative reduction in internal layer power remains past the end of melt season and does not recover by December (Figure 3a). The englacial water did not locally refreeze or drain throughout the observational period since the loss of liquid water would reduce the englacial attenuation signal. Thermal observations and theoretical models support the idea that englacial water can remain liquid for long periods of time up to months or years (Forster et al., 2013;

Humphrey et al., 2012; Meyer & Hewitt, 2017). While we do not have data over multiple years to determine how long the liquid water remains stored englacially, the observed echo strengths and seasonal increase in attenuation are inconsistent with many years of accumulated water storage.

To investigate the possibility of multiyear storage, we estimate the maximum amount of melt observable by the ApRES, by analyzing the signal to noise ratio of the radar bed echoes from the processed 2-D radar profiles (Figure 2). We estimate the noise floor is around −70 to −80 dB. Given that the bed power at the start of May is about −28 dB, the maximum power loss possible before the bed echo is lost in noise is roughly 52 dB. This power loss corresponds to a maximum possible amount of storage between 1.4 and 3.5 m of water in a porous layer between 5.1–63.0 m thick, slightly larger than is estimated in this study for 2014. If comparable englacial storage persisted from any previous melt season, it would be unlikely that the ApRES system could have measured the bed echo starting in May of our 2014 deployment. The englacial water system of Store Glacier appears to have a short residence time amounting to a year at the most, with the impounded water likely refreezing or draining to the bed after our observational period between December and early May of the following season.

4.3. Evidence of Subglacial Drainage

The 2-D radar profiles collected by ApRES simultaneously capture radar echoes from both englacial layers and the bed. From the bed echoes, we observe an active subglacial water system throughout both deployments directly beneath the region of englacial water storage. Between May and early June, we observe periodic changes in bed echo power of 10–12 dB, lasting between 11 and 17 days, superimposed on the attenuation signal (Figure 3b). The magnitude of these oscillations is consistent with episodic drainage events through a subglacial water system causing a brighter bed interface as water is routed directly beneath the deployment site (Chu et al., 2016; Peters et al., 2005). From the AWS record, positive temperatures were briefly observed on 8 May while the bulk of melting occurred between 1 June and 9 September. We observe at least two periodic drainage events after 9 May, before the first supraglacial lakes appear in satellite imagery around 1 June (Williamson et al., 2017). Therefore, the initial source of subglacial water appears not to be immediately supraglacial in origin and is either from the drainage of subglacial lakes upstream or from periodic drainage of water stored at the ice-bed interface during the previous winter (Chu et al., 2016; Willis et al., 2015). The transition after 11 June to more sporadic bed power variations and a potentially well-connected subglacial system dependent on surface melt aligns with a sharp increase in surface melting or runoff as suggested by RACMO2.3p2 SMB estimates and persistent AWS temperatures above freezing. Supraglacial lakes are also observed to persist on the ice surface after 10 June (Williamson et al., 2017) and the subglacial drainage of these lakes likely contribute to these sporadic power variations.

No clear local hydraulic connection between the englacial and subglacial systems is observed during our record from May to December. Since all internal layers are equally attenuated, no intermediate features within the ice column linking the englacial water storage to drainage events are apparent in the 2-D ApRES radar profiles. The persistence of the attenuation signal beyond the end of the melt season also suggests water remains stored englacially with no connection to the bed through December. We would expect the drainage of englacial water to be marked by a detectable increase in internal layer power. Given our estimates of maximum water storage in section 4.2 however, it is possible either a subglacial connection develops outside of our observational record or significant refreezing occurs after December.

5. Conclusions

This radiometric time series of phase-sensitive radar sounding observations offers an unprecedented view of the interaction between the englacial and subglacial water drainage systems of the Greenland Ice Sheet. Our results demonstrate that englacial water storage may be a pervasive, yet overlooked feature of ice sheet hydrology, occurring not only in the thick firn layers (Forster et al., 2013) but also in bare ice regions (Cooper et al., 2018). At Store Glacier, englacial water storage can intercept a significant portion of the surface water budget which persists for likely one melt season. Without the incorporation of regional englacial storage delaying a fraction of the surface melt water from reaching the bead, model-based assessments of the Greenland Ice Sheet will not fully capture the dynamic response to surface melt water input. Our observations also indicate that the englacial water storage at Store Glacier is locally disconnected from the subglacial drainage during the melt season, which contrasts with studies in Southwest Greenland where vertical

recharge from englacial storage does reach the bed (Miller et al., 2017; Poinar et al., 2017). If such recharge occurs at Store Glacier, it would have to occur during the late winter, potentially leading to a dampening of seasonal variations in basal lubrication and flow (Schoof, 2010). Therefore, glacial hydrology models that do not include varied and evolving englacial water systems are unlikely to capture the role of surface melt in ice sheet behavior, stability, and sea-level contribution.

Acknowledgments

D. M. S. and W. C. were partially supported by a grant from the NASA Cryospheric Sciences Program. Collection of the ApRES data was supported by the University of Cambridge Fieldwork Funds and by the UK Natural Environmental Research Council (NERC) grant NE/K006126, awarded to T. J. Y. and P. C., respectively. S. H. D. was funded by NERC grant NE/K005871/1. A. H. acknowledges a professorial fellowship funded by the Research Council of Norway through its Centres of Excellence (grant 223259). L. B. L. is supported by a University Research Fellowship from The Royal Society. Geospatial support for this work provided by the Polar Geospatial Center under NSF-OPP awards 1043681 and 1559691. DEMs were provided by the Polar Geospatial Center under NSF OPP awards 1043681, 1559691, and 1542736. Landsat-8 image courtesy of the U.S. Geological Survey. We thank Joe Todd and Marion Bougamont for assistance in choosing the field site, the crew of SV Gambo for logistical support, Ann Andreasen and the Uummannaq Polar Institute for local support, and Coen Hofstede for assistance in the field. We also thank two anonymous reviewers for their constructive comments. The code used to estimate water storage is available for download from https://www.doi.org/10.5281/zenodo.1323920. The internal layer power and AWS data used are available from https://www.doi.org/10.6084/m9.figshare.7104368. Modeled crevasse depth is available from http://doi.org/chg7. RACMO2.3p2 data are available without conditions from Noël et al., 2018.

References

Aglyamov, Y., Schroeder, D. M., & Vance, S. D. (2017). Bright prospects for radar detection of Europa's ocean. *Icarus*, *281*, 334–337. https://doi.org/10.1016/j.icarus.2016.08.014

Andrews, L. C., Catania, G. A., Hoffman, M. J., Gulley, J. D., Lüthi, M. P., Ryser, C., et al. (2014). Direct observations of evolving subglacial drainage beneath the Greenland ice sheet. *Nature*, *514*(7520), 80–83. https://doi.org/10.1038/nature13796

Bartholomew, I., Nienow, P., Sole, A., Mair, D., Cowton, T., & King, M. A. (2012). Short-term variability in Greenland ice sheet motion forced by time-varying meltwater drainage: Implications for the relationship between subglacial drainage system behavior and ice velocity. *Journal of Geophysical Research*, *117*, F03002. https://doi.org/10.1029/2011JF002220

Bohren, C. F., & Huffman, D. R. (1983). *Absorption and scattering of light by small particles*. New York: Wiley. https://doi.org/10.1017/S0263574798270858

Brennan, P. V., Nicholls, K., Lok, L. B., & Corr, H. (2014). Phase-sensitive FMCW radar system for high-precision Antarctic ice shelf profile monitoring. *IET Radar, Sonar and Navigation*, *8*(7), 776–786. https://doi.org/10.1049/iet-rsn.2013.0053

Chu, W., Schroeder, D. M., Seroussi, H., Creyts, T. T., Palmer, S. J., & Bell, R. E. (2016). Extensive winter subglacial water storage beneath the Greenland ice sheet. *Geophysical Research Letters*, *43*, 12,484–12,492. https://doi.org/10.1002/2016GL071538

Clarke, P. S., Orton, J. W., & Guest, A. J. (1978). Electrical-conductivity and Hall-effect measurements in semiconducting powders. Study of percolation effects. *Physical Review B*, *18*(4), 1813–1817. https://doi.org/10.1103/PhysRevB.18.1813

Cooper, M. G., Smith, L. C., Rennermalm, A. K., Miège, C., Pitcher, L. H., Ryan, J. C., et al. (2018). Meltwater storage in low-density near-surface bare ice in the Greenland ice sheet ablation zone. *The Cryosphere*, *12*(3), 955–970. https://doi.org/10.5194/tc-12-955-2018

Cuffey, K. M., & Paterson, W. S. B. (2010). *The physics of glaciers* (4th ed.). Burlington, MA: Elsevier Science.

Doyle, S. H., Hubbard, B., Christoffersen, P., Young, T. J., Hofstede, C., Bougamont, M., et al. (2018). Physical conditions of fast glacier flow: 1. Measurements from boreholes drilled to the bed of store glacier, West Greenland. *Journal of Geophysical Research: Earth Surface*, *123*, 324–348. https://doi.org/10.1002/2017JF004529

Fitzpatrick, A. A. W., Hubbard, A., Joughin, I., Quincey, D. J., As, D. V. A. N., Mikkelsen, A. P. B., et al. (2013). Ice flow dynamics and surface meltwater flux at a land-terminating sector of the Greenland ice sheet. *Journal of Glaciology*, *59*(216), 687–696. https://doi.org/10.3189/2013JoG12J143

Forster, R. R., Box, J. E., van den Broeke, M. R., Miège, C., Burgess, E. W., van Angelen, J. H., et al. (2013). Extensive liquid meltwater storage in firn within the Greenland ice sheet. *Nature Geoscience*, *7*(2), 95–98. https://doi.org/10.1038/ngeo2043

Geldsetzer, T., Langlois, A., & Yackel, J. (2009). Dielectric properties of brine-wetted snow on first-year sea ice. *Cold Regions Science and Technology*, *58*(1–2), 47–56. https://doi.org/10.1016/j.coldregions.2009.03.009

Hooke, R. L. B. (2005). *Principles of glacier mechanics* (2nd ed.). Cambridge, UK: Cambridge University Press. https://doi.org/10.1017/CBO9780511614231

Humphrey, N. F., Harper, J. T., & Pfeffer, W. T. (2012). Thermal tracking of meltwater retention in Greenland's accumulation area. *Journal of Geophysical Research*, *117*, F01010. https://doi.org/10.1029/2011JF002083

Joughin, I., Das, S. B., Flowers, G. E., Behn, M. D., Alley, R. B., King, M. A., et al. (2013). Influence of ice-sheet geometry and supraglacial lakes on seasonal ice-flow variability. *The Cryosphere*, *7*(4), 1185–1192. https://doi.org/10.5194/tc-7-1185-2013

Joughin, I., Smith, B., Howat, I., & Scambos, T. 2015, updated 2017. MEaSUREs Greenland ice sheet velocity map from InSAR data, *Version 2* [2014-2015]. Boulder, Colorado USA. NASA National Snow and Ice Data Center Distributed Active Archive Center. https://doi.org/10.5067/OC7B04ZM9G6Q. 2017-10-04

Kingslake, J., Hindmarsh, R. C. A., Aðalgeirsdóttir, G., Conway, H., Corr, H. F. J., Gillet-Chaulet, F., et al. (2014). Full-depth englacial vertical ice sheet velocities measured using phase-sensitive radar. *Journal of Geophysical Research: Earth Surface*, *119*, 2604–2618. https://doi.org/10.1002/2014JF003275

Koenig, L. S., Miège, C., Forster, R. R., & Brucker, L. (2014). Initial in situ measurements of perennial meltwater storage in the Greenland firn aquifer. *Geophysical Research Letters*, *41*, 81–85. https://doi.org/10.1002/2013GL058083

Leuschen, C. (2014). updated 2018. IceBridge MCoRDS L1B geolocated radar echo strength profiles, *Version 2* [2014]. Boulder, Colorado USA. NASA National Snow and Ice Data Center Distributed Active Archive Center. 2018-02-12. https://doi.org/10.5067/90S1XZRBAX5N

MacGregor, J. A., Li, J., Paden, J. D., Catania, G. A., Clow, G. D., Fahnestock, M. A., et al. (2015). Radar attenuation and temperature within the Greenland ice sheet. *Journal of Geophysical Research: Earth Surface*, *120*, 983–1008. https://doi.org/10.1002/2014JF003418

MacGregor, J. A., Winebrenner, D. P., Conway, H., Matsuoka, K., Mayewski, P. A., & Clow, G. D. (2007). Modeling englacial radar attenuation at Siple Dome, West Antarctica, using ice chemistry and temperature data. *Journal of Geophysical Research*, *112*, F03008. https://doi.org/10.1029/2006JF000717

Matsuoka, K., MacGregor, J. A., & Pattyn, F. (2012). Predicting radar attenuation within the Antarctic ice sheet. *Earth and Planetary Science Letters*, *359-360*, 173–183. https://doi.org/10.1016/j.epsl.2012.10.018

Matsuoka, K., Morse, D., & Raymond, C. F. (2010). Estimating englacial radar attenuation using depth profiles of the returned power, central West Antarctica. *Journal of Geophysical Research*, *115*, F02012. https://doi.org/10.1029/2009JF001496

Mätzler, C. (2002). MATLAB functions for mie scattering and absorption. *IAP Res Rep* (Vol. 2002–08). Institut für Angewandte Physik. Retrieved from http://arrc.ou.edu/~rockee/NRA_2007_website/Mie-scattering-Matlab.pdf

Meyer, C. R., & Hewitt, I. J. (2017). A continuum model for meltwater flow through compacting snow. *The Cryosphere*, *11*(6), 2799–2813. https://doi.org/10.5194/tc-11-2799-2017

Miège, C., Forster, R. R., Brucker, L., Koenig, L. S., Solomon, D. K., Paden, J. D., et al. (2016). Spatial extent and temporal variability of Greenland firn aquifers detected by ground and airborne radars. *Journal of Geophysical Research: Earth Surface*, *121*, 2381–2398. https://doi.org/10.1002/2016JF003869

Miller, O. L., Solomon, D. K., Miège, C., Koenig, L., Forster, R. R., Montgomery, L. N., et al. (2017). Hydraulic conductivity of a firn aquifer in southeast Greenland. *Frontiers in Earth Science*, *5*, 38. https://doi.org/10.3389/FEART.2017.00038

Montgomery, L. N., Schmerr, N., Burdick, S., Forster, R. R., Koenig, L., Ligtenberg, S., et al. (2017). Investigation of firn aquifer structure in southeastern Greenland using active source seismology. *Frontiers in Earth Science*, *5*, 10. https://doi.org/10.3389/FEART.2017.00010

Moon, T., Joughin, I., Smith, B., van den Broeke, M. R., van de Berg, W. J., Noël, B., & Usher, M. (2014). Distinct patterns of seasonal Greenland glacier velocity. *Geophysical Research Letters*, *41*, 7209–7216. https://doi.org/10.1002/2014GL061836

Nicholls, K. W., Corr, H. F. J., Stewart, C. L., Lok, L. B., Brennan, P. V., & Vaughan, D. G. (2015). Instruments and methods: A ground-based radar for measuring vertical strain rates and time-varying basal melt rates in ice sheets and shelves. *Journal of Glaciology*, *61*(230), 1079–1087. https://doi.org/10.3189/2015JoG15J073

Noël, B., Van De Berg, W. J., Van Wessem, J. M., Van Meijgaard, E., Van As, D., Lenaerts, J. T. M., et al. (2018). Modelling the climate and surface mass balance of polar ice sheets using RACMO2—Part 1: Greenland (1958-2016). *The Cryosphere*, *12*(3), 811–831. https://doi.org/10.5194/tc-12-811-2018

Peters, M. E., Blankenship, D. D., & Morse, D. L. (2005). Analysis techniques for coherent airborne radar sounding: Application to West Antarctic ice streams. *Journal of Geophysical Research*, *110*, B06303. https://doi.org/10.1029/2004JB003222

Poinar, K., Joughin, I., Lilien, D., Brucker, L., Kehrl, L., & Nowicki, S. (2017). Drainage of Southeast Greenland Firn aquifer water through crevasses to the bed. *Frontiers in Earth Science*, *5*, 1–15. https://doi.org/10.3389/feart.2017.00005

Schoof, C. (2010). Ice-sheet acceleration driven by melt supply variability. *Nature*, *468*(7325), 803–806. https://doi.org/10.1038/nature09618

Schroeder, D. M., Blankenship, D. D., Raney, R. K., & Grima, C. (2015). Estimating subglacial water geometry using radar bed echo specularity: Application to Thwaites glacier, West Antarctica. *IEEE Geoscience and Remote Sensing Letters*, *12*(3), 443–447. https://doi.org/10.1109/LGRS.2014.2337878

Segelstein, D. J. (1981). The complex refractive index of water. *M.S. Thesis*. University of Missouri, Kansas City. Retrieved from http://hdl.handle.net/10355/11599

Smith, L. C., Chu, V. W., Yang, K., Gleason, C. J., Pitcher, L. H., Rennermalm, A. K., et al. (2015). Efficient meltwater drainage through supraglacial streams and rivers on the southwest Greenland ice sheet. *Proceedings of the National Academy of Sciences of the United States of America*, *112*(4), 1001–1006. https://doi.org/10.1073/pnas.1413024112

Sole, A. J., Mair, D. W., Nienow, P. W., Bartholomew, I. D., King, M. A., Burke, M. J., & et al. (2011). Seasonal speedup of a Greenland marine-terminating outlet glacier forced by surface melt–induced changes in subglacial hydrology. *Journal of Geophysical Research*, *116*, F03014. https://doi.org/10.1029/2010JF001948

Todd, J., Christoffersen, P., Zwinger, T., Raback, P., Chauché, N., Råback, P., et al. (2018). A full-stokes 3D calving model applied to a large Greenland glacier. *Journal of Geophysical Research: Earth Surface*, *123*, 410–432. https://doi.org/10.1002/2017JF004349

Ulaby, F. T., Long, D. G., Blackwell, W. J., Elachi, C., Fung, A. K., Ruf, C., et al. (2014). *Microwave radar and radiometric remote sensing*, (Vol. 4). Ann Arbor: University Of Michigan Press. https://doi.org/10.3998/0472119356

Warren, S. G., & Brandt, R. E. (2008). Optical constants of ice from the ultraviolet to the microwave: A revised compilation. *Journal of Geophysical Research*, *113*, D14220. https://doi.org/10.1029/2007JD009744

Williamson, A. G., Arnold, N. S., Banwell, A. F., & Willis, I. C. (2017). A fully automated supraglacial lake area and volume tracking ("FAST") algorithm: Development and application using MODIS imagery of West Greenland. *Remote Sensing of Environment*, *196*, 113–133. https://doi.org/10.1016/j.rse.2017.04.032

Willis, M. J., Herried, B. G., Bevis, M. G., & Bell, R. E. (2015). Recharge of a subglacial lake by surface meltwater in northeast Greenland. *Nature*, *518*(7538), 223–227. https://doi.org/10.1038/nature14116

Young, T. J., Schroeder, D. M., Christoffersen, P., Lok, L. B., Nicholls, K. W., Brennan, P. V., et al. (2018). Resolving the internal and basal geometry of ice masses using imaging phase-sensitive radar. *Journal of Glaciology*, *64*(246), 649–660. https://doi.org/10.1017/jog.2018.54

Zwally, H. J., Abdalati, W., Herring, T., Larson, K., Saba, J., & Steffen, K. (2002). Surface melt-induced acceleration of Greenland ice-sheet flow. *Science*, *297*(5579), 218–222. https://doi.org/10.1126/science.1072708